Title
TISSUE ACTIVATION STUDIES WITH ALPHA PARTICLE BEAMS

Authors
Maccabee, H.D.
Madhvanath, U.
Raju, M. R.

Publication Date
1968-06-15

University of California

Ernest O. Lawrence

Radiation Laboratory

TISSUE ACTIVATION STUDIES WITH ALPHA PARTICLE BEAMS

H. D. Maccabee, U. Madhvanath, and M. R. Raju

June 15, 1968

Berkeley, California

DISCLAIMER

To be submitted to
Physics in Medicine and Biology

UCRL-17929
Preprint

UNIVERSITY OF CALIFORNIA

Lawrence Radiation Laboratory
Berkeley, California

AEC Contract No. W-7405-eng-48

TISSUE ACTIVATION STUDIES WITH ALPHA PARTICLE BEAMS

H. D. Maccabee, U. Madhvanath, and M. R. Raju

June 15, 1968

UCRL-17929

Tissue Activation Studies with Alpha Particle Beams

H. D. MACCABEE,† M. S., Ph. D.

U. MADHVANATH, B. Sc., M. A.

and

M. R. RAJU,* M. A., M. Sc., D. Sc.

Donner Laboratory, University of California
Lawrence Radiation Laboratory, Berkeley, California

†Present address: M. R. C. Radiobiological Research Unit, Harwell, Didcot, Berkshire.
*Associate Professor: Southwest Center for Advanced Studies, Dallas, Texas.

1. Introduction

When a fast particle passes through tissue, there is a certain probability that a nuclear interaction will occur with a nucleus of the medium, and that the product nucleus will be radioactive. Tissue activation was first discussed by Tobias (1947) and Tobias and Dunn (1949). Nuclear reactions initiated by positively charged particles often leave a nucleus which has too many protons for stability, and therefore tends to decay by positron emission. Examples of such reactions include (p, γ), (p, d), (p, n), $(p, 2n)$, (d, n), (d, t), (α, n), $(\alpha, 2n)$, and $(\alpha, \alpha n)$. Charged particle activation has been reviewed by Tilbury and Wahl (1965) and Tilbury (1966). Since many such activation reactions are endoergic, the incoming particle must have not only enough kinetic energy to penetrate the Coulomb barrier (2 to 5 MeV in light elements), but also enough to meet the Q-value for the reaction. For alpha particles of energy greater than 25 MeV, total cross sections for such reactions in carbon, nitrogen, and oxygen may be as large as 500 mb. Thus when an energetic alpha particle beam passes through tissue, as in medical irradiation, it leaves behind a weak trail of radioactive nuclei, mostly short-lived positron and γ-ray emitters.

Some of the important alpha particle activation reactions in tissue are shown in Table 1, along with the modes of decay of the radioactive product nuclei. The maximum energy of the emitted particle spectrum is given above the arrow, and the decay half-life is given below the arrow. Data are taken from Lederer, Hollander, and Perlman (1967).

The most important characteristic of the positron decay process, for our purposes, is the fact that when the positron reaches the end of

its range, it annihilates with a negative electron to form a γ-ray pair with equal energies (0.51 MeV each) and nearly opposite momenta. Simple coincidence methods may be used to locate the point of annihilation by simultaneous detection of the γ-ray pair. This is the basis of the activation studies to be discussed in the following sections.

2. Positron decay curves

Our first approach to the alpha particle activation phenomenon was to irradiate tissue and its components in the 53 MeV alpha beam of the Berkeley 88-inch sector-focussed cyclotron, and measure the decay curves of the positron-emitting activated species. In a typical experiment, the sample was irradiated for 3 minutes in the cyclotron beam, with a beam current of 0.1 millimicroampere, then removed and placed in an automatic counting system. The detection system consists of a pair of NaI (Tl) scintillators aligned opposite to one another, with associated electronics. When both scintillators simultaneously detect a 0.511 MeV γ-ray pair from positron annihilation, the resulting coincidence pulse is fed to a scaler and a pulse-height analyser in the time-dwell mode, so that the time-dependent positron decay rate may be automatically recorded.

The simplest tissue component examined in this manner was carbon, in the form of a graphite slug; the results of this experiment are shown in fig. 1. The decay curve has two main components. After about 20 minutes, the predominant decay mode has a half-life of 20.3 minutes, corresponding well to the isotope ^{11}C, which has a known half-life of 20.3 minutes, and indicating the reaction $^{12}_{6}C\ (\alpha, \alpha n)\ ^{11}_{6}C \xrightarrow{\beta^+} {}^{11}_{5}B$. The earlier decay rate, after subtraction of the extrapolated 20.3-minute

activity, yields a half-life of 2 minutes. This corresponds to the isotope $^{15}_{8}O$, whose known half-life is 123 seconds, and indicates the reaction $^{12}_{6}C(\alpha, n)^{15}_{8}O \xrightarrow{\beta^+} {}^{15}_{7}N$.

The results of the irradiation of soft tissue (beef muscle) are shown in fig. 2. Note that after the ^{11}C activity dies away, the primary activity is that of ^{18}F, corresponding to the reaction $^{16}_{8}O(\alpha, pn)^{18}_{9}F \xrightarrow{\beta^+} {}^{18}_{8}O$. The measured half-life of 115 minutes is in fairly good agreement with the known figure of 110 minutes. This observed activity is the main result of the fact that tissue contains oxygen and other elements, in addition to carbon. Other activities were not observed because of their shorter half-lives (they decay away before they were placed in the detector), smaller reaction cross-sections, and lower abundance of the target isotope in tissue.

We have noted that the 20.3-minute activity of ^{11}C is predominant at times from 10 minutes to 1 hour after irradiation. For reasons which become evident in the next section, this time period is of primary importance, and therefore the reaction $^{12}C(\alpha, \alpha n)^{12}C$ merits closer examination. The cross section for this reaction has been measured by Lindner and Osborne (1953) and Crandall, Millburn, Pyle and Birnbaum (1956).

The energy dependence of the cross section is plotted in fig. 3. The cross section rises steeply from the threshold at 22 MeV, and is relatively constant at around 50 mb over a wide energy range up to 380 MeV. This behaviour is typical of many charged-particle activation reactions, that is, rising quickly from a threshold to a broad plateau and then gradually falling off due to competition from other reactions. Thus the activation behaviour of a charged monoenergetic heavy particle beam

in matter is likely to be a relatively uniform distribution along the track, which drops abruptly to nothing when the residual range of the particles decreases to that corresponding to the threshold energy of the reaction. In the case of fast alpha particles in tissue, all $^{12}C(\alpha, \alpha n)^{11}C$ reactions cease at 0.5 mm (0.02 in.) from the end of the track. The sharpness of this effect is tempered, however, by the initial energy spread of the beam as well as by energy straggling in the absorbing material.

3. Phantom studies

C. A. Tobias has suggested that it might be possible to visualize and locate the Bragg ionization peak of a positively charged particle beam by observing the variation in positron activation at the end of the beam track. With this idea in mind, we irradiated several plastic phantoms with 910 MeV alpha particles from the 184-inch Berkeley synchrocyclotron, and then observed the activation pattern in the positron scintillation camera, as developed by H. O. Anger (Anger and Rosenthal 1959 and Anger 1963). The positron camera uses an image detector and a focal detector aligned on opposite sides of the subject, along with coincidence circuitry and electronic coordinate computation techniques, to produce an image of the positron annihilations within a subject. The image is in the form of dots on a cathode-ray tube, and may be photographed to yield a picture of the activation pattern.

Fig. 4 shows a schematic diagram of an experiment in which fast alphas were stopped in a Lucite phantom, and a picture of the resulting activation pattern. The 910 MeV beam was collimated through a 1/2-inch round aperture and then passed through a 1.34-inch-thick copper absorber, reducing the residual beam energy to approximately 510 MeV, and then absorbed in the plastic block. After 20 000 rads (air dose at entry) were

delivered, the block was removed from the cyclotron area and transported to the positron camera. Because of time lost in transportation, the picture shown (1 minute exposure) was taken 20 minutes after the end of irradiation; thus, the predominant positron activity is due to the $^{12}C(\alpha, \alpha n)^{11}C \xrightarrow[20.3\,m]{\beta^+} {}^{11}B$ reaction. The initial coincidence count rate was 10 500 per minute, and the estimated activity of the block after 30 minutes was 20 μCi.

By taking scintiphotos of reference sources separated by a known distance, calibration of the length in the positron camera pictures is possible. Using this calibration, the length of the activation track due to 510 MeV alphas in Lucite was measured to be 3.98 ± 0.08 inches. This compares well with the calculated length, 3.98 inches (4.00 in. range minus 0.02 in.) The transverse "fuzzing out" of the beam track is due to multiple scattering and the longitudinal variation is due to range and energy straggling of the beam; even if these effects were not present, the picture would be blurred by the inherent resolution of the positron camera itself, which we discuss in a following section. The background dots in the portion of the Lucite block not associated with the beam track are believed to be due to $^{12}C\,(n, 2n)^{11}C \xrightarrow{\beta^+} {}^{11}B$ reactions caused by background neutrons emanating from (α, n) reactions.

On the basis of a further experiment in which the alpha beam was completely stopped and the positron activity due to the (putatively) neutron background was observed alone, it was found that the background activity amounted to roughly 10% of the activity due to the charged particles. If one assumes that the (n, 2n) cross section is approximately equal to the $(\alpha, \alpha n)$ cross section in our situation, the conclusion is that the

total neutron intensity incident on the phantom is roughly 10% of the alpha particle intensity. Most of these neutrons, however, are believed to be due to nuclear reactions in the brass collimator and copper absorber, and are not believed to be associated with the cyclotron alpha beam itself.

Despite these side effects, it is clear that this technique makes it possible to visualize and locate the end of the track of a positively charged particle beam in matter. At the penetration corresponding to the Bragg ionization peak of a 910 MeV alpha beam, the modal energy of the alpha particles is approximately 85 MeV (Raju, 1967). The range-energy relation can then be used to predict that the Bragg peak is expected to occur about 4 mm "upstream" of the end of the activation track.

In the next experiment we attempted to discern the activation pattern resulting from the transmission of 910 MeV alpha beams in a situation similar to that of a patient irradiation. We used a paraffin head phantom irradiated with 2000 rads in each of three ports, separated by 1.3 inches caudally and staggered by 1 cm in the A-P direction. The collimator aperture was 1 cm by 1 cm square, and the phantom was rotated 70° about only one axis transverse to the beam. Fig. 5 shows the irradiation scheme and the photographic results of the experiment. The nonuniformity of the activation images in intensity and lateral extent is due to the fact that the phantom was placed in the scintillation camera with the Lucite holder mask and aluminum rotator adaptor still attached, and these parts added an extra activation pattern of their own (superimposed upon and collinear with that of the paraffin). It is apparent that the activation pattern gives enough separation and geometric resolution to provide good information as to the course of the beam in tissue-like

material. The width of the "hot spots" in the original photo was measured to be 1.1 cm, which corresponds well with the collimator opening of 1 cm.

4. Patient studies

The final experiments in this series were designed to determine the activation pattern resulting from the actual irradiation regime of a patient being treated by the Donner Laboratory method of pituitary ablation by rotational superposition of transmitted 910 MeV alpha beams. Fig. 6 illustrates the method of the rotational irradiation; the head is held in a plastic mask molded to the shape of the face and rotated by a system of automatically controlled servo-mechanisms, 70° about the x-axis and 66° about the y-axis, with the beam axis aligned roentgenographically to pass through the pituitary at all times.

In a typical single sitting of an acromegalic case (A. I.), 760 rads were administered through a 3/4-inch circular aperture. After the end of irradiation the patient was transported from the cyclotron medical cave to Donner Laboratory and positioned in the positron camera, taking 14 minutes. Fig. 7 illustrates the irradiation scheme used in this case, and gives an A-P view of the positron decays recorded in 8 minutes, yielding a total of 2320 counts. The edges of the expected "butterfly" activation pattern are moderately well delineated, but the "hot spot" expected at the vertex (corresponding to the pituitary) is not clearly evident, probably due to biological "washout", i. e. transport of ^{11}C away from the site. It is clear, however, that this technique can be used to visualize the activation pattern (and, therefore, the dose distribution) of a positively charged particle beam in an irradiated patient. A similar picture has been obtained by Malcolm Powell (private communication,

University of California Medical Center, San Francisco, 1968).

5. Possible applications

We envision several possible applications of the technique of tissue activation with radiation beams. Perhaps the most natural application would be the use of the positron camera as an on-line alignment tool for patient therapy with the Bragg peak of positively charged heavy particle beams. (See, for example, Kjellberg, Koehler, Preston, and Sweet, 1963, or Gottschalk, 1963). Since alignment in the (x-y) plane transverse to the beam axis is already very good with conventional methods, the important parameter to be controlledis penetration of the beam along the beam axis (the "z" coordinate). In other words, because of variation of density and composition of tissue, bone, sinuses, etc., it is difficult to predict exactly at what depth the Bragg peak will occur. Koehler, Dickinson, and Preston (1965) give a different solution to the problem. Using the activation technique, however, it might be possible to visualize the end of the beam track (and, therefore, determine the Bragg peak depth) with the administration of a few rads, and adjust the beam energy so that the peak would coincide exactly with the volume to be irradiated (e.g., tumour, pituitary, etc.). The rest of the treatment dose could then be completed. This method imposes three requirements on the activation visualization system: 1) the activation camera must be "on-line," i.e., with detectors in the treatment cave, and with fast readout; 2) the spatial resolution of the activation camera must be such that it could be used to align the beam end with sufficient accuracy (e.g., ± 3 mm) in a small target; 3) the sensitivity of the activation camera must be such that it produces a usable picture with a small alignment dose (e.g., 30 rads or less).

The first requirement is not difficult: the only problem envisioned is that of shielding the detectors or discriminating in some way against

the background radiation present in the treatment cave. The second and third questions, resolution and sensitivity, have been examined in detail by Anger(1966 a), and we only make a few comments on the subject. One of the inherent limitations on the positron activation camera is the fact that a 1 MeV positron has a range of about 4.3 mm in soft tissue before it is annihilated to form the γ-ray pair which is detected. There are two factors which mitigate this effect, however. First, the positrons are emitted with a continuous "beta" energy distribution, whose maximum energy is given by the values shown in Table 1; the mean energy of the distribution is about 1/3 of the maximum; and, therefore, the mean range of the positrons is less than 1/3 of the maximum. The second factor is that the positrons are emitted isotropically in the three spatial dimensions: x, y, z; if we let r equal the radial penetration of the positron, $r^2 = x^2 + y^2 + z^2$, and by isotropy, z^2 (mean) = 1/3 r^2 (mean). Since dispersion in the x and y directions are unimportant when we are considering penetration in the z-direction, we are left with the conclusion that the root-mean-square pentration of the positron in the x-direction before annihilation is given by z (rms) $\approx$ 0.58 r (mean). The net result is that a 1 MeV (max) positron spectrum contributes less than 1 mm to the resolution of the image in the direction of the beam axis. This contribution is thus small compared with the contribution of the NaI crystal and phototube detection array (about 5 mm), but there are several possibilities of improving the inherent detector resolution (Anger 1966b).

In light of the fact that 760 rads in a patient's head produced a picture with 2320 dots in 8 minutes exposure after about 18 minutes delay from beam shut-off, one might surmise that it would be impossible

to get a useful picture with only 30 rads. This is not so, however; if the positron camera were "on-line" in the irradiation cave, and could be turned on immediately after beam shut-off, the much higher activity due to ^{15}O ($T_{1/2}$ = 123 sec) could be detected, and a much smaller dose would produce a useful picture. One can calculate, for example, that 30 rads of stopping alpha particles would leave an initial positron activity of about 0.15 μCi. Since the existing positron camera sensitivity is adequate to produce 2000 picture dots per minute from 1 μCi (Anger 1966 a), 30 rads could produce 300 dots per minute initially, and estimating that 600 dots can make a useful picture for z-direction alignment purposes, this could be accomplished with a 2 minute exposure. Thus, an "on-line" positron camera with slight improvement in sensitivity and a factor of 2 improvements in resolution could be a useful alignment and diagnostic tool for charged particle radiation therapy.

5.1 Other applications

A natural extension of the idea of visualising the activation due to heavy charged particle beams is the possibility of visualizing other beams. Recently there has been much discussion of using other heavy particle beams for therapy, including pi mesons, neutrons, and very heavy ions, for reasons of higher LET, lower OER, and better depth-dose distribution. It is likely that the (n, 2n) reactions occurring from neutron beams will leave a good amount of positron activity in tissue. Unquestionably, heavy ion beams will leave activity very similar to that of the alpha particle beams discussed above.

It might even be possible to visualise the activity from existing therapeutic electron accelerators, such as betatrons and linacs, with

beam energies greater than 20 MeV. The γ-ray bremsstrahlung can cause activation in tissue; for example, the cross section for the $^{12}C(\gamma, n)^{11}C$ reaction in carbon is 10 mb at 20 MeV (Tilbury 1965).

There have been several other interesting suggestions for the use of tissue activation techniques (Sargent 1962 and Biomedical Studies 1967). If a microbeam of particles were incident on a part of an organism or a cell organelle (e.g., a chloroplast), activation analysis techniques might be used to determine the location and amount of trace metals, etc. In vivo activation analysis with charged particles might prove useful for quantitative determination of tissue constituents. Also, tracer studies with short-lived radionuclides might be expedited by generating the radionuclides within an organ of the body, using a particle beam, or even by implanting radioactive ions in the body.

ACKNOWLEDGMENTS

We wish to thank Edward J. Lampo and Frank T. Upham for help with detection and electronics, Hal O. Anger for the use of the positron camera, and Cornelius A. Tobias for his encouragement and the suggestion of using the positron activation detection technique for locating the Bragg peak of heavy charged particles. Dr. Maccabee wishes to thank the U. S. Atomic Energy Commission for postdoctoral fellowship support.

SUMMARY

We have studied the positron-emitting activation of tissue by alpha particle beams, by using the annihilation γ-ray coincidence detection technique, and the Anger positron camera. We have measured the decay spectrum in tissue following irradiation by 53 MeV alphas from the Berkeley 88-inch cyclotron, and visualized the activation pattern resulting from a 910 MeV alpha particle beam stopping in a tissue-like plastic phantom, at the Berkeley 184-inch synchrocyclotron. Also studied were the activation patterns resulting from transmission of 910 MeV alpha beams through a wax head phantom, and the activation pattern in patients' heads resulting from one sitting of the pituitary ablation therapy technique.

With slight improvements in resolution and sensitivity, an "on-line" positron camera technique could be useful for alignment of the end of the beam track in Bragg peak therapy with heavy charged particles. There are other novel applications which might be possible, using tissue activation techniques.

Table I. Important alpha particle activation reactions in tissue.

$^{12}_{6}C(\alpha, \alpha n)$	$^{11}_{6}C$	$\xrightarrow[20.3\ min]{\beta^+\ 0.97\ MeV}$	$^{11}_{5}B$
$^{12}_{6}C\ (\alpha, n)$	$^{15}_{8}O$	$\xrightarrow[123\ sec.]{\beta^+\ 1.74\ MeV}$	$^{15}_{7}N$
$^{12}_{6}C\ (\alpha, 2n)$	$^{14}_{8}O$	$\xrightarrow[71\ sec]{\beta^+\ 1.81\ MeV}$	$^{14}_{7}N$
$^{16}_{8}O\ (\alpha, pn)$	$^{18}_{9}F$	$\xrightarrow[110\ min]{\beta^+\ 0.635\ MeV}$	$^{18}_{8}O$
$^{16}_{8}O\ (\alpha, \alpha n)$	$^{15}_{8}O$	$\xrightarrow[123\ sec]{\beta^+\ 1.74\ MeV}$	$^{15}_{7}N$
$^{16}_{8}O\ (\alpha, n)$	$^{19}_{10}Ne$	$\xrightarrow[17.4\ sec]{\beta^+\ 2.22\ MeV}$	$^{19}_{9}F$
$^{14}_{7}N\ (\alpha, \alpha n)$	$^{13}_{7}N$	$\xrightarrow[9.96\ min]{\beta^+\ 1.20\ MeV}$	$^{13}_{6}C$
$^{14}_{7}N\ (\alpha, n)$	$^{17}_{9}F$	$\xrightarrow[66\ sec]{\beta^+\ 1.74\ MeV}$	$^{17}_{8}O$

REFERENCES

ANGER, H. O., and ROSENTHAL, D. J., 1959, Medical Radioisotope Scanning (Vienna: IAEA), p. 59.

ANGER, H. O., 1963, Nucleonics, 21 (10) 56.

ANGER, H. O., 1966 a, IEEE Trans. Nucl. Sci., NS-13 (3) 380.

ANGER, H. O., 1966 b, ISA Trans., 5, 311.

Biomedical Studies with Heavy Ion Beams, 1967, Lawrence Radiation Laboratory Report UCRL-17357. See especially, articles by C. A. TOBIAS et al., p. 108, R. M. LEMMON, p. 101, W. E. SIRI et al., p. 273, D. C. VAN DYKE, p. 278, T. W. SARGENT, p. 281.

CRANDALL, W. E., MILLBURN, G. P., PYLE, R. V., and BIRNBAUM, W., 1956, Phys. Rev., 101, 329.

GOTTSCHALK, A., LYMAN, J. T. and McDONALD, L. W., 1963, Lawrence Radiation Laboratory Report UCRL-11184, p. 121.

KJELLBERG, R. N., KOEHLER, A. M., PRESTON, W. M., and SWEET, W. H., 1963, in Second International Symposium on the Response of the Nervous System to Ionizing Radiation.

KOEHLER, A. M., DICKINSON, V. G. and PRESTON, W. M., 1965, Rad. Res., 26, 334.

LEDERER, C. M., HOLLANDER, J. M., and PERLMAN, I., 1967, Table of Isotopes (New York: Wiley).

LINDNER, M., and OSBORNE, R. N., 1953, Phys. Rev., 91, 1501.

RAJU, M. R., 1967, Rad. Res. Suppl., 7, 43.

SARGENT, T. W., 1962, Whole Body Counting (Vienna: IAEA) p. 447

TILBURY, R. S., and WAHL, W. H., 1965, Nucleonics, September.

TILBURY, R. S., 1966, Activation Analysis with Charged Particles, Natl. Acad. Sci.-Nat. Res. Council Report NAS-NS-3110.

TOBIAS, C. A., 1947, AECD-2099B.

TOBIAS, C. A., and DUNN, R. W., 1949, Science 109, 109.

FIGURE LEGENDS

Fig. 1. Positron decay spectrum of carbon after irradiation by 53-MeV Alpha particles.

Fig. 2. Positron decay spectrum of soft tissue after irradiation by 53 MeV alpha particles.

Fig. 3. Energy-dependent cross section for the reaction ^{12}C (α, αn) ^{11}C.

Fig. 4. Diagram of method and scintiphotograph of activation pattern resulting from 910 MeV alpha particle beam stopping in Lucite phantom.

Fig. 5. Diagram of method and scintiphotos of activation pattern resulting from 910 MeV alpha beams transmitted through rotating paraffin wax head phantom.

Fig. 6. Photograph of subject in head holder-rotator used in pituitary ablation technique, illustrating rotation axes and beam axis.

Fig. 7. Diagram of rotation technique and scintiphoto of positron activation resulting from one sitting (760 rads) of pituitary ablation therapy.

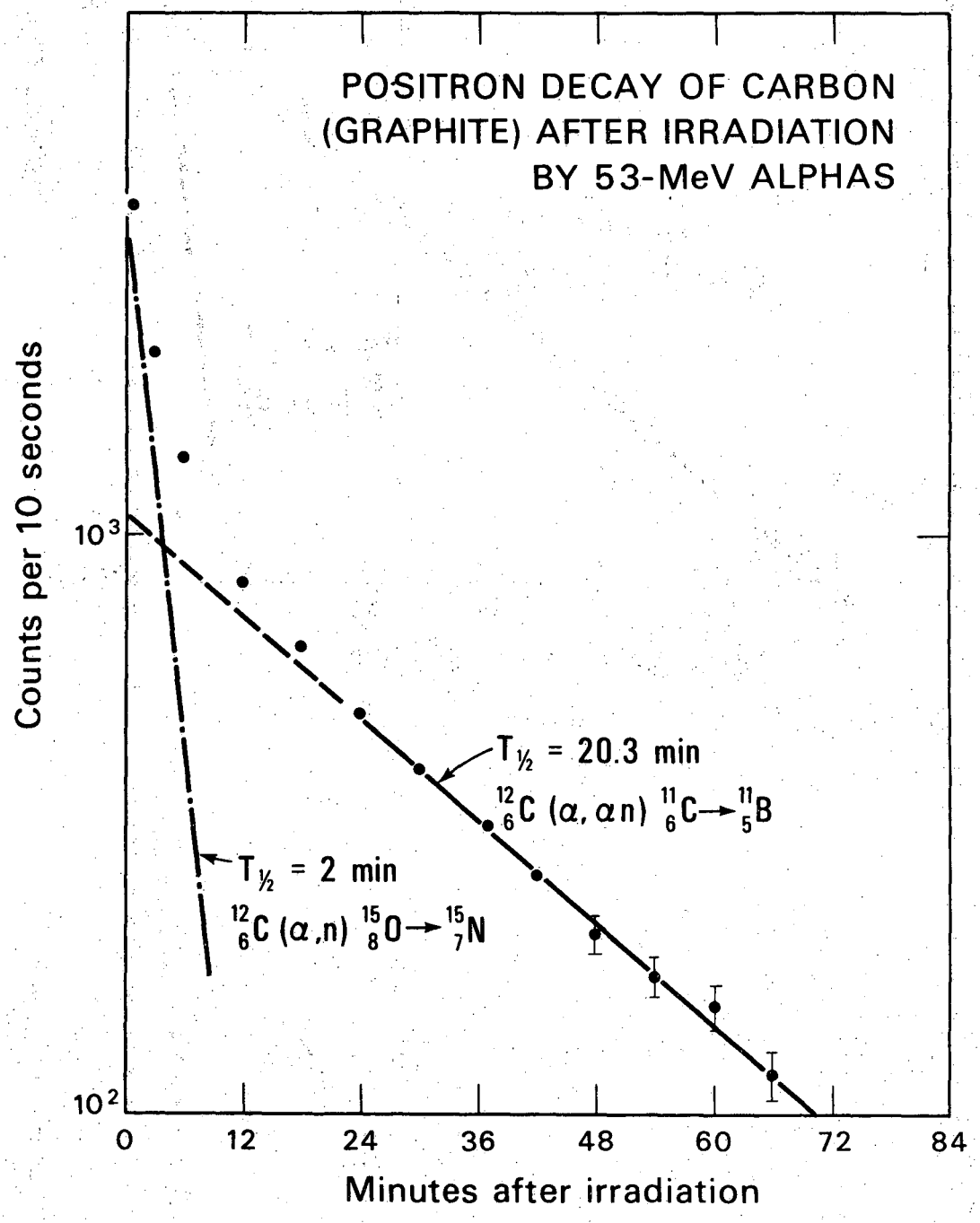

Fig. 1 DBL 6711-1869

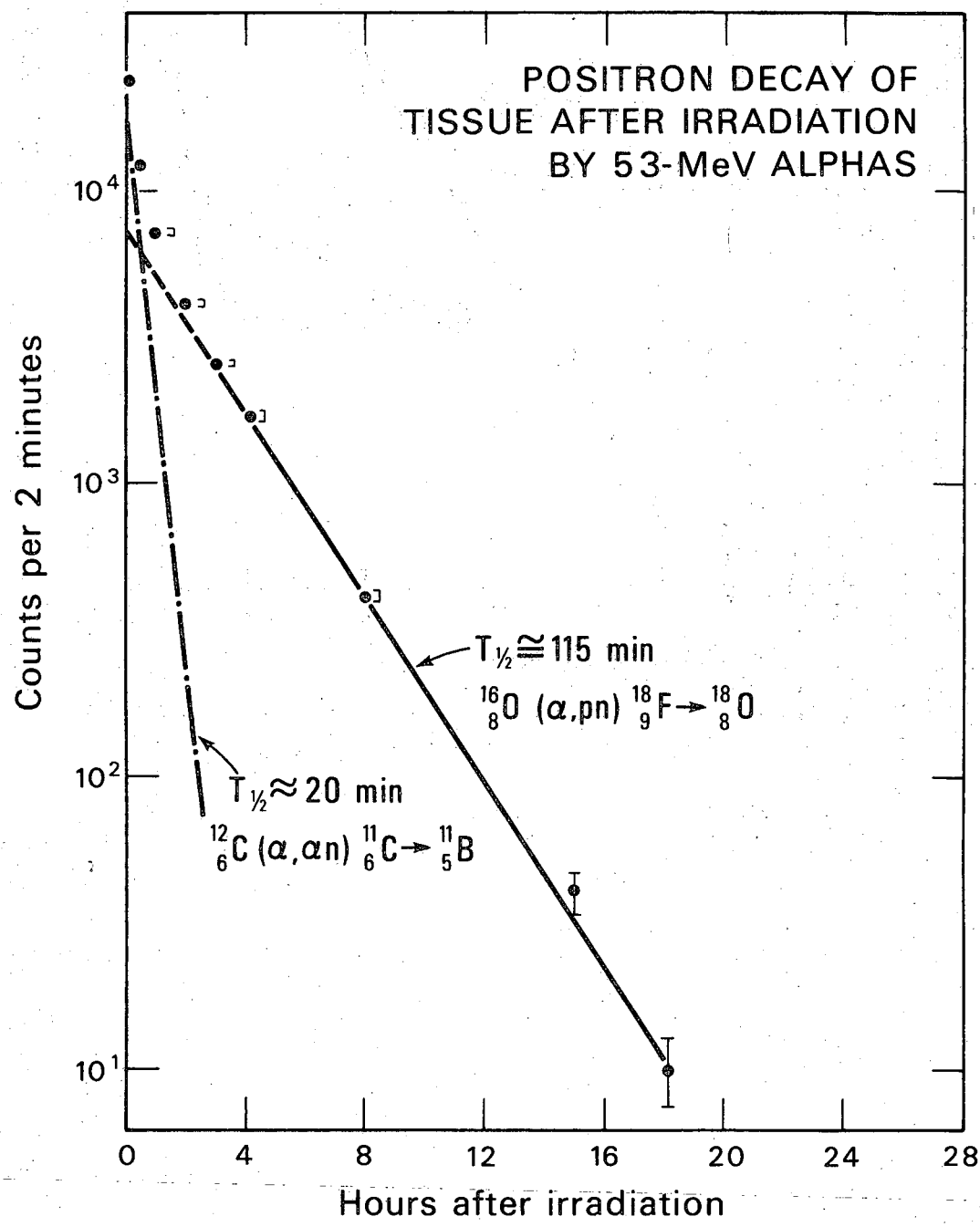

Fig. 2

DBL 6711-1867

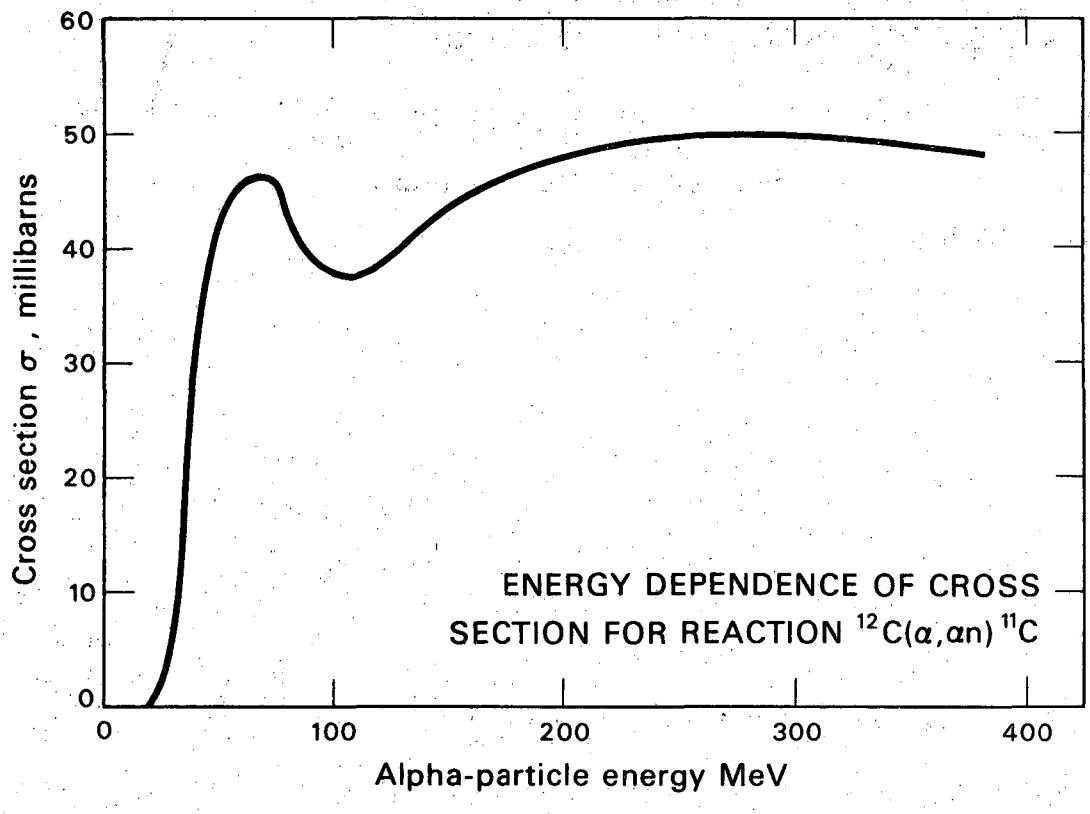

Fig. 3

DBL 6711-1868

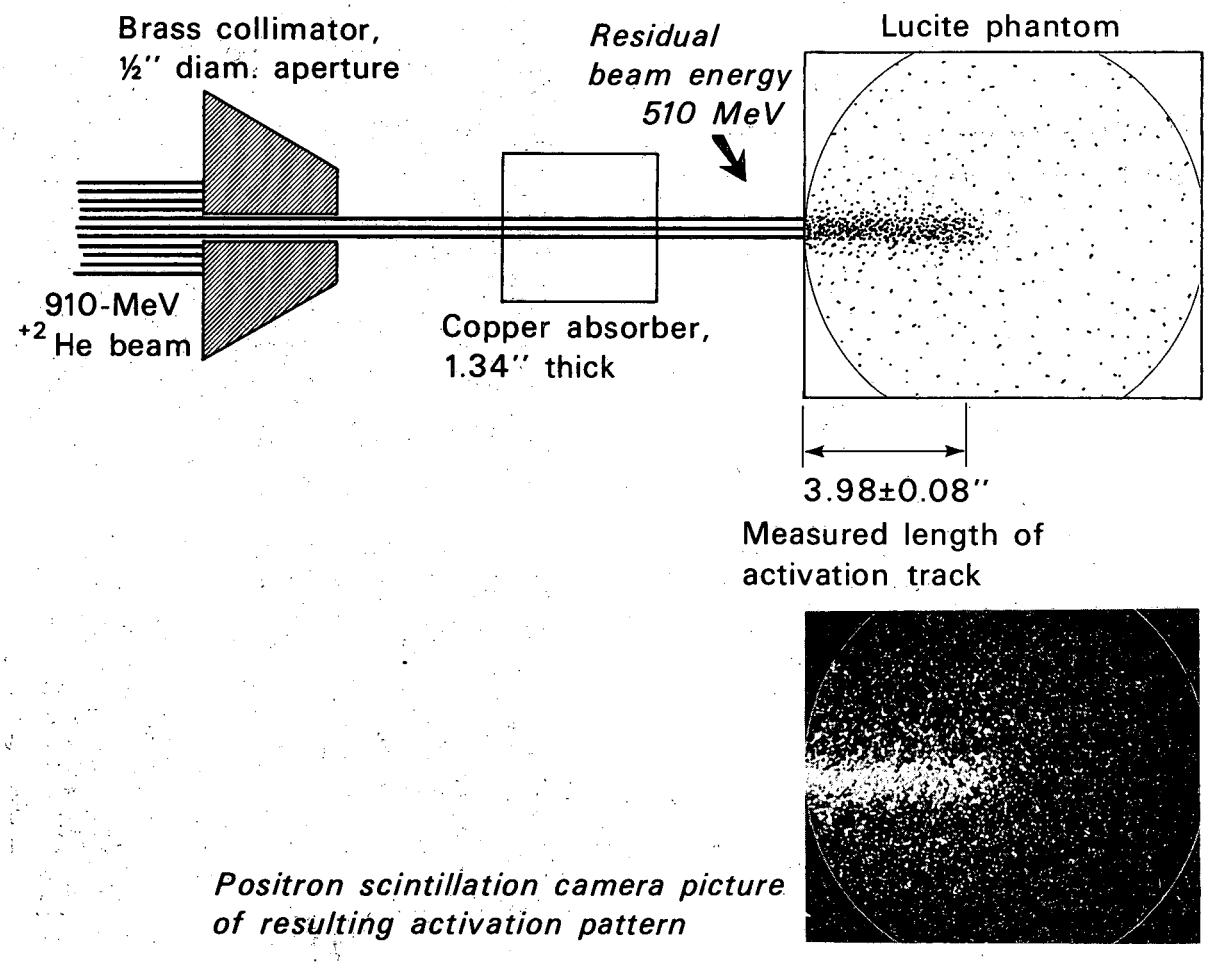

XBB 6711-6558

Fig. 4

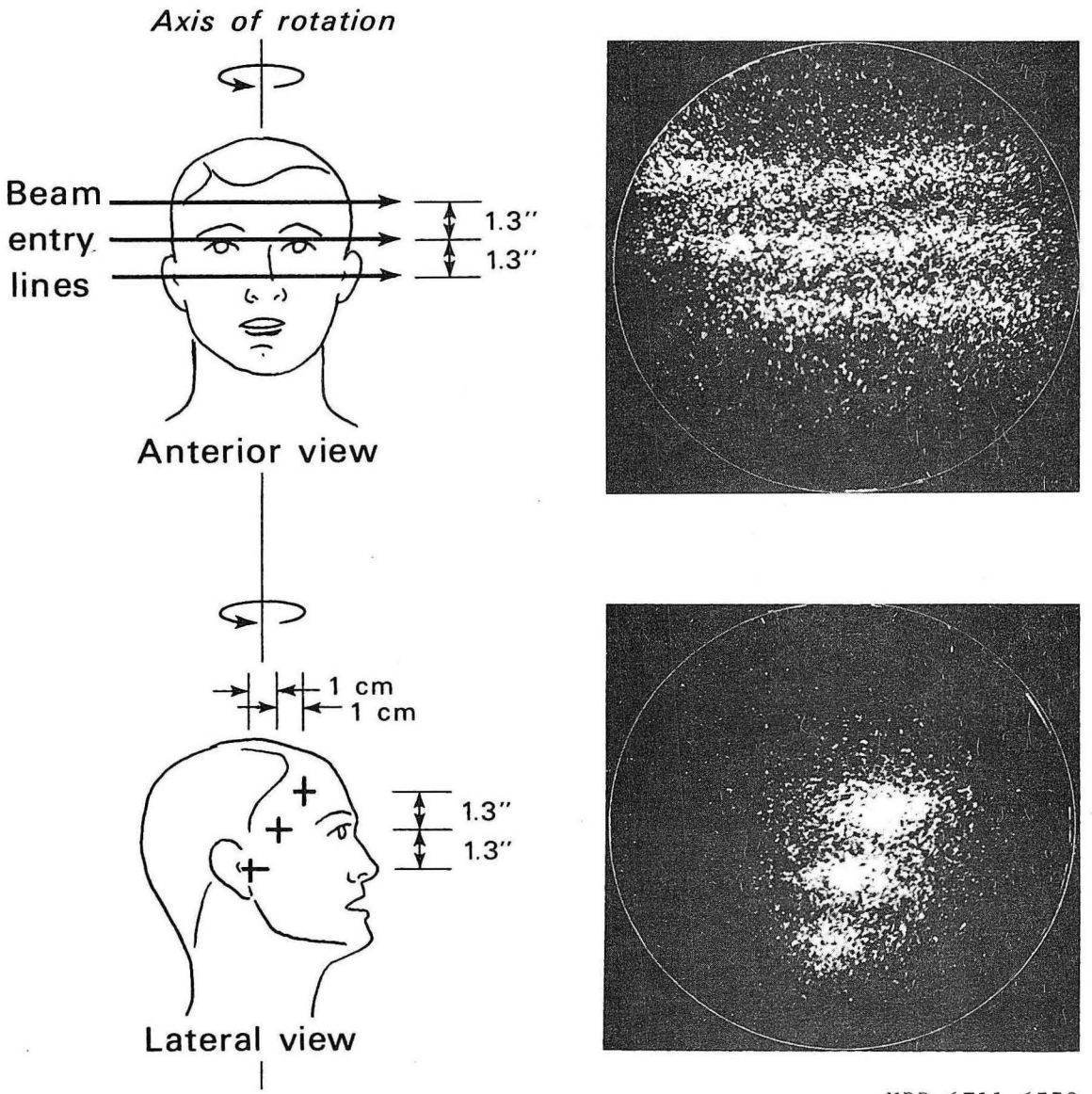
Axis of rotation
Beam entry lines
1.3"
1.3"
Anterior view
1 cm
1 cm
1.3"
1.3"
Lateral view
XBB 6711-6559

Fig. 5

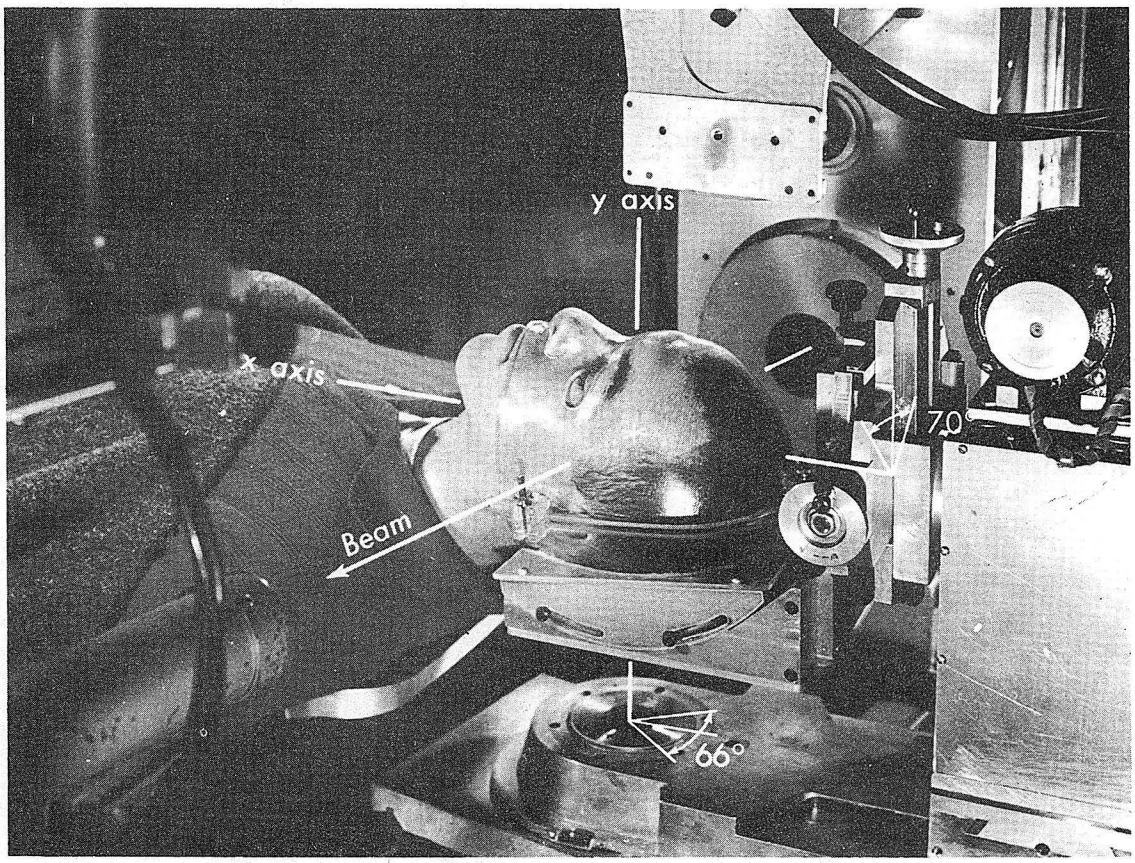

JHL 2897-A

Fig. 6

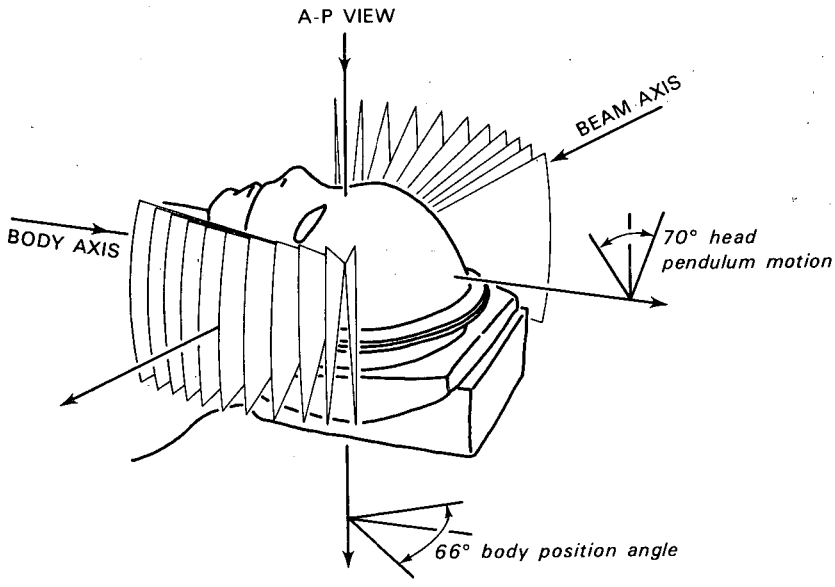

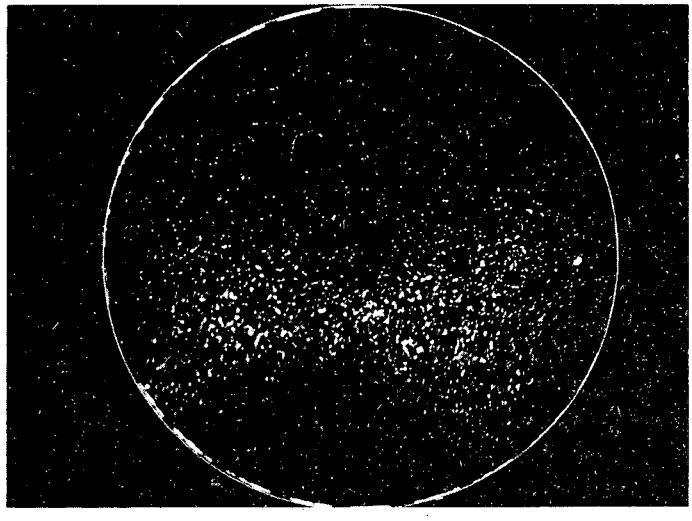

POSITRON ACTIVATION (A-P view)

XBB 6711-6560

Fig. 7